Soft Computing (2022) 26:3789–3808
https://doi.org/10.1007/s00500-022-06767-9

OPTIMIZATION

An advanced Grey Wolf Optimization Algorithm and its application to planning problem in smart grids

Bahman Ahmadi[1] · Soheil Younesi[1] · Oguzhan Ceylan[2,3] · Aydogan Ozdemir[1]

Accepted: 10 January 2022 / Published online: 1 February 2022

Abstract

Due to the complex mathematical structures of the models in engineering, heuristic methods which do not require derivative are developed. This paper improves recently developed Grey Wolf Optimization Algorithm by extending it with three new features: namely presenting a new formulation for evaluating the positions of search agents, applying mirroring distance to the variables violating the limits, and proposing a dynamic decision approach for each agent either in exploration or exploitation phases. The performance of Advanced Grey Wolf Optimization (AGWO) method is tested using several optimization test functions and compared to several heuristic algorithms. Moreover, a planning problem in smart grids is solved by considering different objective functions using 33 and 141 bus distribution test systems. From the numerical simulation results, we observe that, AGWO is able to find the best results compared to other methods from 10 and 9 out of 13 test functions for 30 and 60 variables, respectively. Similar to this, it finds best function values for 5 out of 10 fixed number of variable test functions. Also, the result of the CEC-C06 2019 benchmark functions shows that AGWO outperforms 8 for optimization problems from 10. In power distribution system planning problem, better objective function values were determined by using AGWO, resulting a better voltage profile, less losses, and less emission costs compared to solutions obtained by Grey Wolf Optimization (GWO) and Particle Swarm Optimization (PSO) algorithms.

Keywords Optimization algorithm · Evolutionary computation · Smart grid applications · Renewable energy integration

1 Introduction

Meta-heuristic algorithms are derivative-free and problem-independent methods that solve optimization problems. Although they cannot guarantee global optimal solutions, they become prevalent due to their advantages over analytical methods. Some of their advantages are ease of application, fast convergence, reliable, and robust performance. Moreover, the probability of being trapped in the local minimum points can be reduced, and their global search capability can be increased to find global solutions. These algorithms have been successfully and widely applied to so many problems in different domains.

Meta-heuristic algorithms can be used for single or multi-objective optimization purposes. During the last decades, using different inspirations either from natural processes, physics, and so on, different evolutionary optimization algorithms (EOAs) were developed. EOAs mainly use swarm intelligence methods to obtain the optimal or near-optimal points in the search space. Some of the popular EOAs are Genetic Algorithms (GA) (Whitley 1994), Particle Swarm Optimization (PSO) (Trelea 2003), Differential Evolution (DE) (Qin et al. 2009), Cuckoo Search (CS) (Yang and Deb 2009), and Grey Wolf Optimization Algorithm (GWO) (Mirjalili et al. 2014). Research on the development of new algorithms continues; for example, the heat transfer relation-

✉ Oguzhan Ceylan
oguzhan.ceylan@khas.edu.tr ;
oguzhan.ceylan@marmara.edu.tr

Bahman Ahmadi
ahmadi18@itu.edu.tr

Soheil Younesi
younesi19@itu.edu.tr

Aydogan Ozdemir
ozdemiraydo@itu.edu.tr

[1] Department of Electrical Engineering, Istanbul Technical University, Istanbul, Turkey

[2] Management and Information Systems Department, Kadir Has University, Istanbul, Turkey

[3] Department of Electrical and Electronics Engineering, Marmara University, Istanbul, Turkey

based optimization algorithm (HTOA) (Asef et al. 2021), the search space reduction (SSR) (Mahesh and Sushnigdha 2021), and the arithmetic optimization algorithm (AOA) (Abualigah et al. 2021) have been recently proposed for the optimization of global optimization problems. Abualigah et al. (2021) proposed the algorithm named Aquila Optimizer (AO), inspired by the behavior of aquilas in nature during prey capture.

Usually, EOAs are based on natural phenomena, social behavior, hunting behavior, and animals' biological behavior. GA (Whitley 1994) was the first evolutionary-based algorithm based on the natural process of evolution through reproduction. GAs can solve complex and non-linear problems; however, the algorithm may get stuck in local minimums Burke and Kendall (2005). PSO is one of the well-known swarm-based algorithms, where each solution is considered as a particle with specific characteristics for defining the particle's moving direction (Eberhart and Kennedy 1995). PSO cannot escape from local optimal points in a high-dimensional search space, and therefore, its convergence rate is low. GWO (Mirjalili et al. 2014) is a newly introduced meta-heuristic algorithm, which intends to formulate the group hunting behavior of grey wolves. The preliminary studies (Mirjalili et al. 2014, 2016; Mirjalili 2015) show that the GWO algorithm is very promising and could outperform existing population-based algorithms, such as GA, PSO, and DE algorithms, in various applications. The main advantages of GWO algorithm compared to other population-based algorithms are as follows: It is easier to implement, and not many parameters to be set. On the other hand, the method may fall into local minimum points while attacking the prey, and the convergence speed may slow down in the long period of the optimization process.

EOAs have been applied to solve many convex and non-convex problems in different fields. Global optimization problems were solved in Zhu et al. (2015); Saremi et al. (2015); Shehab et al. (2019); Boveiri and Elhoseny (2018); Gupta and Deep (2020); Chu et al. (2020); Elaziz et al. (2020), and portfolio optimization problem was solved in Bavarsad Salehpoor and Molla-Alizadeh-Zavardehi (2019). Nguyen et al. optimized artificial neural networks (ANNs) using PSO to predict ground surface response for short buildings (Nguyen et al. 2020). One of the popular EOA applications in health sciences aims to support decision making systems. For example, image processing techniques based on optimized ANNs have been proposed to support a lung disease detection system (Ke et al. 2019). Optimization of switching angles of multilevel inverters (Ceylan 2020; Rahmani et al. 2014; Gnana Sundari et al. 2016) and optimal speed control of a brushless DC motor (Premkumar and Manikandan 2015) are some examples from power electronics. There are also several EOA applications in power systems. Some examples are optimal power flow considering the stochastic turbines and flexible alternating current transmission system devices (Nguyen and Vo 2018), dynamic economic load dispatch (Kansal and Dhillon 2020), siting and sizing of shunt capacitors and energy resources in radial distribution systems (Biswas et al. 2017), and so on.

Determining optimal locations and sizes of Distributed Generators (DGs) and Energy Storage Systems (ESSs) directly impacts on the performance of the distribution grids in power systems. Hence, for a reliable and efficient system, this planning problem needs to be solved. If the DGs' optimal locations and sizes cannot be appropriately determined, loss minimization, voltage profile improvement, or any other intended objectives cannot be optimized. In the literature, GWO was used to reduce the energy losses and improve voltage profiles by solving a weighted combination of these objectives in Sultana et al. (2016). There were other studies focused on the minimization of the active power losses in the branches using GWO (Sanjay et al. 2017; Arabi Nowdeh et al. 2019; Ahmadi et al. 2019a). There were also other EOAs applied to determine the optimal numbers, locations, and sizes of DGs. Some of them include quasi-oppositional chaotic symbiotic organisms search algorithm (Truong et al. 2019, 2020), the modified symbiotic organisms' search algorithm (Saha and Mukherjee 2020), multiobjective version of multiverse optimization algorithm (Ahmadi et al. 2021), and the hybrid version of particle swarm optimization (Tolba Mohamed et al. 2020). Other power system problems were solved using heuristic algorithms. A recent paper (Saha et al. 2020) aimed to solve the transient stability constrained optimal power flow problem using a novel hybrid differential evolution and symbiotic organism search algorithm (HSOS). Intentional islanding problem was solved by oppositional crow search optimizer (OCSO). The study implemented the algorithm on a 69-bus test system considering various factors such as the constraints of line capacity, bus voltage, load priority controllability, and the capability of integrating the islands to produce higher intentional islands (Karthikumar and Kumar 2021). A detailed review of meta-heuristic methods implemented in smart grid problems can be found in Papadimitrakis et al. (2021).

Several advanced and modified versions of the GWO were developed to find better near-optimal solutions and to alleviate the disadvantages of GWO method in solving optimization problems. Most of these algorithms aimed to find a better balance between exploitation and exploration. For instance, in Khandelwal et al. (2018), the authors tried to modify the GWO to improve the capability of smoothly balancing between the exploration and exploitation phases. In other words, they updated positions of δ wolves with the help of existing δ and ω wolves (the position variable is the average of the δ and ω position variable). In Salgotra et al. (2019), an extended version of GWO based on enhancing the exploration phase capabilities was proposed. As known, the

classical GWO uses the fittest three members for updating the agent positions. A recent study defines the fourth fittest member as Gamma and uses it together with alpha, beta, and delta wolves to direct Omega wolves in determining optimal weight and bias values of a recurrent neural network to predict student performance (Rashid et al. 2019). To improve the performance, one approach may be to use higher number of fittest members (for instance five or seven fittest members). However, since more information will be used for update operation, the convergence rate may decrease; thus, the required number of iterations to converge to near optimal results will increase. Moreover, the requirement of performing more calculations will result in an increase in computational time.

In Heidari and Pahlavani (2017), a novel modified version of GWO with levy flight is developed to boost the efficiency of GWO. In Mahdad and Srairi (2015), GWO was hybridized with a pattern search algorithm (PSA) aiming to reduce the risk of blackouts in the power systems where PSA was used as a local search mechanism to improve the balance between the exploration and the exploitation phases of the GWO. The resulting GWO-PSA method provided fewer blackouts in the power system under critical conditions. Another hybridizing was done with differential evolution (DE) method (Zhu et al. 2015), focusing on jumping out of the stagnation with DE's exploration searching ability.

The authors of (Yang et al. 2017) proposed the Grouped GWO algorithm (GGWO) by dividing the population of grey wolves into two parts. The first group members play a role in the hunting of prey and the second group is used to randomly explore the search space. The numerical results of GGWO (Yang et al. 2017) on solving the test functions were compared to those of GA, PSO, GWO, and Moth-flame Optimization (MFO) (Mirjalili 2015). It was observed that the results were improved by merely adding a second group of grey wolves.

From the available studies, which aimed to improve the GWO, one can easily see that falling into the local optimum points, and weak exploration phases are still vital problems because search agents in GWO always update their positions according to only the top three fittest members of the group. The other members do not play a substantial role in generating a new solution and thus making the algorithm stuck in local optimum points.

The main contributions of this study are follows.

- We propose Advanced Grey Wolf Optimization Algorithm (AGWO) to improve the performance of conventional GWO for the solution of Smart Grid Planning Problem. The most important modifications are as follows:
  - AGWO uses a new formulation to determine the position of the search agents. It brings a bidirectional acting ability providing a balance between exploration and exploitation phases.
  - The AGWO checks the boundaries of the positions using a symmetry-based mirroring distance which assures that the position values are always within the feasible ranges.
  - AGWO provides a dynamic guidance for the search agents to make up their decision on evaluating either in the exploitation phase or in the exploration phase.
- We validate the performance of the AGWO algorithm by optimizing several test functions used in the relevant literature (Mirjalili et al. 2014, 2016; Price et al. 2018) and compared with of the GWO, PSO, Ant Lion Optimizer (ALO) (Mirjalili 2015), Salp Swarm Optimization Algorithm (SSA) (Mirjalili et al. 2017), and Harmony Search (HS) (Geem et al. 2001) methods.
- We apply the AGWO to a smart grid optimization problem, since we assume that obtaining a better objective function value through the implementation has a positive impact on the physical performance of the power distribution system, by incurring less power losses and thus improving the economic operating conditions. In this regard, we solve a non-convex mixed-integer nonlinear programming (MINLP) type planning problem in smart grids using four different objective functions, such as improving voltage profiles, minimizing losses, minimizing emission costs of thermal power plants, and minimizing a hybrid cost function, which is the linear combination of the previous three objectives. The proposed formulation and solution algorithm are tested on two well-known distribution test systems (IEEE 33- and 141-bus radial distribution systems) for different load and DG output scenarios. The numerical results are compared with those obtained using classical GWO and PSO.

The structure of the paper is as follows. We give an overview of GWO in Sect. 2. Then, the proposed AGWO concept and its methodology are provided in Sect. 3. We model optimization test functions and smart grid planning problems in Sect. 4 and implement the AGWO algorithm. Section 5 shows the simulation results of optimization test functions and smart grid optimization models. Conclusions are given in Sect. 6.

2 An overview of Grey Wolf Optimization Algorithm

GWO (Mirjalili et al. 2014) was proposed by Mirjalili in 2014. Grey wolf is a predator at the top of the food chain; the

group hunting behavior of grey wolves in nature is the main inspiration to develop this optimization algorithm. Group members are divided into four different types, and each wolf has its specific role in the population. The alpha (α) is the leader and is mainly responsible for making decisions about hunting; the beta (β) is responsible for assisting the leader in managing other group members. The delta (δ) wolves are mainly responsible for watching the boundaries of the territory and warning others from the dangers. The fourth types are the omega (ω) wolves which follow other types of wolves. The hunting process is composed of three phases: encircling the prey, hunting the prey, and attacking the prey.

In the encircling the prey phase, the grey wolf can update its position inside the search space around the prey in any random location. This behavior is mathematically modeled as follows:

$$\vec{X}_{(t+1)} = \vec{X}_p - \vec{A}.|\vec{C}.\vec{X}_p - \vec{X}_{(t)}| \quad (1)$$

$$\vec{A} = 2.a.\vec{r}_1 - a \quad (2)$$

$$a = 2 - 2 \times \frac{t}{\mathrm{Max}_t} \quad (3)$$

$$\vec{C} = 2.\vec{r}_2 \quad (4)$$

where t and Max_t denote the current iteration and the maximum number of iterations, respectively. In the equations, $\vec{X}_p$ shows a vector that represents the position of prey, and $\vec{X}$ shows a vector corresponding to the position of the grey wolf. The term $\vec{a}$ linearly decreases from 2 to 0 throughout iterations and simulates the behavior of chasing the prey and $\vec{r}_1$, $\vec{r}_2$ are random vectors in the range from 0 to 1.

Grey wolves can identify the position of the prey and encircle them. Then, in the hunting phase, the α types guide the group. The hunting phase is mathematically modeled as follows:

$$\vec{X}_{(t+1)} = \frac{\vec{X}_1 + \vec{X}_2 + \vec{X}_3}{3} \quad (5)$$

where $\vec{X}_1$, $\vec{X}_2$, and $\vec{X}_3$ are the updated positions of a grey wolf considering the position variables of α, β, and δ wolves in Eq. (1) instead of the positions of the prey. Since α, β, and δ have a better knowledge of of the prey locations, they can be used in estimating the positions of preys. After determining the position of the prey, the ω wolves update their states around the estimated location of prey.

In the last phase of the hunting process, the final situation is achieved when prey stops moving. This stage is very important to escape stagnation in local minimum, and it is the most critical disadvantage of the GWO algorithm. The flowchart of GWO algorithm is shown in Fig. 1.

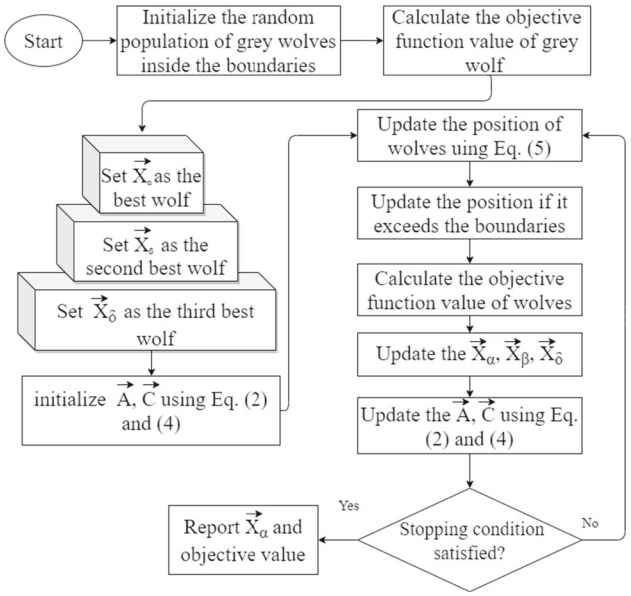

Fig. 1 GWO flowchart m

3 Advanced Grey Wolf Optimization Algorithm

In order to improve the performance of the GWO algorithm and cover the mentioned disadvantages, we propose an advanced version of the GWO algorithm in this section. The AGWO algorithm aims to improve the disadvantages of GWO using the following ideas:

1. It applies a dynamic method to evaluate the search agent positions either in the exploitation or in the exploration phases.
2. It adds a new formulation for evaluating the positions of the search agents.
3. It checks the boundaries of the evaluated search agent positions and brings the variables back to allowed ranges.

In order to simulate the behavior of grey wolves during hunting, let's assume that there are N wolves and d position variables. The position variables in the search agent change considering the position of prey (assumed as the positions of α, β, and δ wolves) using the three phases of hunting process (encircling, hunting and attacking phases). The evaluation of the the position variables of the wolves is formulated as follows: In the encircling prey phase, the algorithm updates the position of the ω wolves inside the search space around the prey by using the following formulation.

$$\vec{X}_{(t+1)} = \vec{X}_p - \vec{A}.\vec{B}.|\vec{C}.\vec{X}_p - \vec{X_{(t)}}| \quad (6)$$

where t denotes the current iteration, $\vec{X}_p$, and $\vec{X}$ are the vectors that represent the position of prey and position of ω

wolves, respectively. The terms $\overrightarrow{A}$, $\overrightarrow{B}$, and $\overrightarrow{C}$ are coefficient vectors formulated as:

$$\overrightarrow{A} = 2.a.\overrightarrow{r}_1 - a \tag{7}$$

$$\overrightarrow{B} = sin(2\pi \overrightarrow{r}_2) \tag{8}$$

$$a = 2 - 2 \times \frac{t}{\text{Max}_t} \tag{9}$$

$$\overrightarrow{C} = 2.\overrightarrow{r}_3 \tag{10}$$

where a linearly decreases from 2 to 0 over the course of iterations and simulates the behavior of chasing the prey; the terms $\overrightarrow{r_1}$ and $\overrightarrow{r_2}$ are random vectors between 0 and 1. The term of $\overrightarrow{B}$ is a sinusoidal function that is dependent on the $\overrightarrow{r}_2$ value, which is between -1 and 1. The ω wolves may either attack the prey or search for another prey, depending upon the value of $\overrightarrow{A}.\overrightarrow{B}$ product. This dual behavior can also be considered as a parameter for improving the exploitation phase of the algorithm. Note that the amount of $\overrightarrow{A}$ in the final iteration will be near to zero and it will simulate the behavior of not moving the prey and it is hunted by the wolves.

Position variables of the search agents are evaluated either in the exploitation phase or the exploration phase based on the formulation given below:

$$ER = b_1 - b_2 \times \frac{t}{\text{Max}_t} \tag{11}$$

$$\overrightarrow{X} = \begin{cases} \overrightarrow{X}_\omega & r_4 \geq ER \\ \overrightarrow{X}_{rand} & r_4 < ER \end{cases} \tag{12}$$

where ER is a dynamically decreasing function that changes from b_1 to $b_1 - b_2$ over the course of iterations which determines the maximum ratio of exploitation phase to the exploration phase; r_4 is a random number between 0 and 1. Since the ER is higher in the beginning of the iterations and lower in the final iterations, the search agent's positions are evaluated more in the exploration phase compared to the final iterations.

Using this method, the global search or exploration phase during the initial iterations and deeply intensive local search or exploitation phase toward the end iterations improves the search abilities and thus avoids falling into local minimums. This method assures a proper balance between the two phases all over the search duration.

In the hunting and attacking phases, the top three objective values of the grey wolves are accepted as the α, β, and δ. Then, the positions of other remaining wolves change related to α, β, and δ position variables using the following equations:

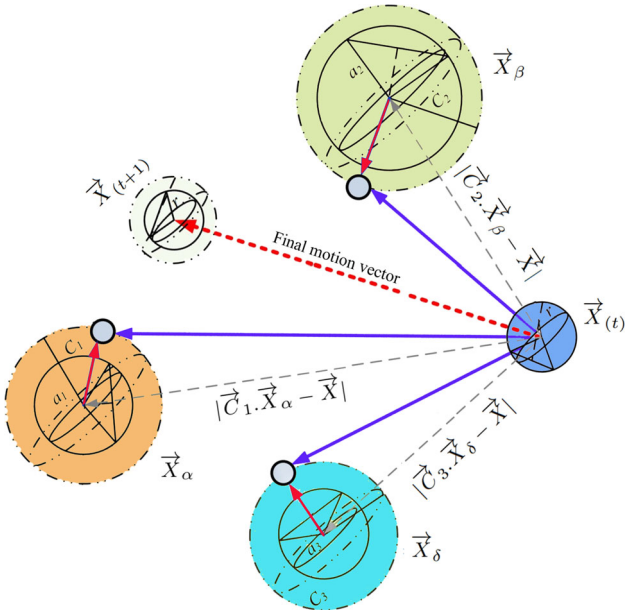

Fig. 2 3D motion of wolves in GWO

$$\overrightarrow{X}_1 = \overrightarrow{X}_\alpha - \overrightarrow{A}_1.\overrightarrow{B}_1.|\overrightarrow{C}_1.\overrightarrow{X}_\alpha - \overrightarrow{X}| \tag{13}$$

$$\overrightarrow{X}_2 = \overrightarrow{X}_\beta - \overrightarrow{A}_2.\overrightarrow{B}_2.|\overrightarrow{C}_2.\overrightarrow{X}_\beta - \overrightarrow{X}| \tag{14}$$

$$\overrightarrow{X}_3 = \overrightarrow{X}_\delta - \overrightarrow{A}_3.\overrightarrow{B}_3.|\overrightarrow{C}_3.\overrightarrow{X}_\delta - \overrightarrow{X}| \tag{15}$$

$$\overrightarrow{X}_4 = \overrightarrow{X} + \overrightarrow{A}_4 \times sin(2\pi \overrightarrow{r}_5).|\overrightarrow{C}_4.\overrightarrow{X}_\alpha - \overrightarrow{X}| \tag{16}$$

$$\overrightarrow{X}_5 = \overrightarrow{X} + \overrightarrow{A}_5 \times cos(2\pi \overrightarrow{r}_6).|\overrightarrow{C}_5.\overrightarrow{X}_\alpha - \overrightarrow{X}| \tag{17}$$

$$\overrightarrow{X}_{\omega(t+1)} = \begin{cases} \frac{\overrightarrow{X}_1 + \overrightarrow{X}_2 + \overrightarrow{X}_3}{3} & r_7 \geq ER \\ \begin{cases} \overrightarrow{X}_4 & r_8 < 0.5 \\ \overrightarrow{X}_5 & r_8 \geq 0.5 \end{cases} & r_7 < ER \end{cases} \tag{18}$$

where $\overrightarrow{X}_\alpha$, $\overrightarrow{X}_\beta$, and $\overrightarrow{X}_\delta$ are the α, β, and δ position vectors.

The search agents' positions are either evaluated using Eqs. (13), (14), and (15) or using Eqs. (16) and (17) decided by r_7 value (randomly generated in between 0 and 1) and ER value. Note that the total number of function evaluations remains same as the GWO.

In the GWO, the α, β, and δ are used to update the positions of remaining members using Eqs. (13), (14), and (15), whereas the positions of search agents in AGWO can also be evaluated using Eqs. (16) and (17). In these two equations, depending on the value of the sinusoidal term and the $\overrightarrow{A}$ vector, the search agent may either move close to or move away from the prey (estimated as the α positions).

In GWO, the movement of wolves is demonstrated in Fig. 2.

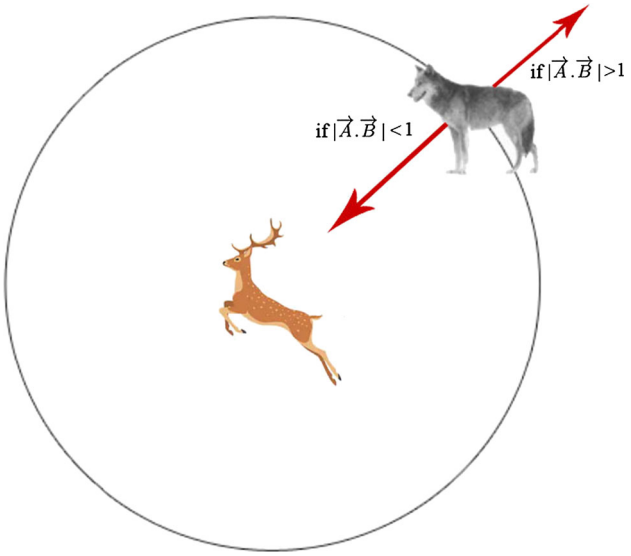

Fig. 3 Dual behavior of ω wolves in AGWO: attacking the prey or searching for another prey

In AGWO, as shown in Fig. 3, the ω wolves may either attack the prey or search for another prey, depending upon the value of $\vec{A}.\vec{B}$ product. This dual behavior can also be considered as a parameter for improving the exploitation phase of the algorithm. Note that the amount of $\vec{A}$ in the final iteration will be close to zero which means that the prey does not move and is hunted by the wolves.

After determining the position of search agents, the boundaries of the positions are checked. They are brought back into the limits by simple arithmetical operations, if they violate the boundaries lb and ub. For instance, if a variable exceeds the upper limit by y, then the new value is set as simply $(\text{ub} - y)$. The pseudo-code is shown in Algorithm 1.

Initialize the random population of grey wolves;
while $t \leq MT$ **do**
  Check the boundaries of search agent position variables using mirroring method;
  Evaluate the fitness value of all search agents;
  Update the X_α as best fitness value;
  Update the X_β as second best fitness value;
  Update the X_δ as third fitness value;
  for *each search agent* **do**
    Update the search agent variables using the Eq. 7-18;
  end
  $t = t + 1$;
  Return the fitness (X_α);
end

Algorithm 1: AGWO algorithm

4 Optimization test functions and smart grid planning problems

Various test functions including convex unimodal, non-convex unimodal, multimodal (non-convex), and discontinuous (Non-Smooth) functions are used to validate the performance and effectiveness of the proposed AGWO algorithm. We tested the performance of the AGWO algorithm on 23 classical benchmark functions (Mirjalili et al. 2014; Mirjalili 2016; Abualigah et al. 2021), 10 CEC-C06 2019 test functions (Price et al. 2018). Moreover, we used four different objective functions to improve the characteristics of the smart grids. The detailed information about the implemented test functions is given in the following subsections. We compared the results to those obtained using GWO, PSO, ALO, SSA, and HS methods.

4.1 Classical benchmark test functions

We use the benchmark functions and formulations provided in Abualigah et al. (2021); Mirjalili et al. (2014). From a total of 23 functions, seven unimodal functions and six multimodal functions were formulated with a high number of dimensions. The mathematical formulation for the problems is shown in Table 1 for unimodal problems and Table 2 for multimodal problems, respectively.

For both unimodal and multimodal problems, the dimensions (variables) of the problem can be determined by the user. For this purpose, we proposed two different dimension scenarios using the variable sizes of 30 and the 60 for each function. For the first scenario of tests, we set the maximum number of iterations as 1000 and for the second scenario as 3000.

The details of the fixed variable sizes of the remaining 10 classical benchmark functions are given in Table 3 where we set the maximum number of iterations to 1000 for solving these functions.

4.2 CEC-C06 2019 benchmark test functions

These test functions are 10 multimodal test functions (Price et al. 2018) designed for IEEE Congress on Evolutionary Computation 2019 (CEC 2019). The variable sizes of test functions 4 to 10 are 10. Test functions 1, 2, and 3 have 9, 16, and 18 variables, respectively. The functions are given in Table 4 (Brest et al. 2019; Abdullah and Ahmed 2019). The maximum number of iteration for CEC test functions was set to 1000.

4.3 Smart grid planning problems

These problems aim to determine the near optimal locations and sizes of DGs and ESSs, to decrease the active power

Table 1 Unimodal benchmark functions

Function	Range	$f_{\min}$
$F_1(x) = \sum_{i=1}^{n} x_i^2$	[−100,100]	0
$F_2(x) = \sum_{i=1}^{n} \lvert x_i \rvert + \prod_{i=1}^{n} \lvert x_i \rvert$	[−10,10]	0
$F_3(x) = \sum_{i=1}^{n} \left(\sum_{j-1}^{i} x_j \right)^2$	[−100,100]	0
$F_4(x) = \max_i \{ \lvert x_i \rvert, 1 \le i \le n \}$	[−100,100]	0
$F_5(x) = \sum_{i=1}^{n-1} \left[100 \left(x_{i+1} - x_i^2 \right)^2 + (x_i - 1)^2 \right]$	[−30,30]	0
$F_6(x) = \sum_{i=1}^{n} [x_i + 0.5]^2$	[−100,100]	0
$F_7(x) = \sum_{i=1}^{n} i x_i^4 + \text{random}[0, 1)$	[−1.28,1.28]	0

Table 2 Multimodal benchmark functions

Function	Range	$f_{\min}$
$F_8(x) = \sum_{i=1}^{n} -x_i \sin\left(\sqrt{\lvert x_i \rvert}\right)$	[−500,500]	-418.9829×5
$F_9(x) = \sum_{i=1}^{n} \left[x_i^2 - 10\cos(2\pi x_i) + 10 \right]$	[−5.12,5.12]	0
$F_{10}(x) = -20\exp\left(-0.2\sqrt{\frac{1}{n}\sum_{i=1}^{n} x_i^2} \right) - y$	[−32,32]	0
$y = \exp\left(\frac{1}{n}\sum_{i=1}^{n} \cos(2\pi x_i)\right) + 20 + e$		
$F_{11}(x) = \frac{1}{4000}\sum_{i=1}^{n} x_i^2 - \prod_{i=1}^{n} \cos\left(\frac{x_i}{\sqrt{1}}\right) + 1$	[−600,600]	0
$F_{12}(x) = z + \sum_{i=1}^{n} u(x_i, 10, 100, 4)$	[−50,50]	0
$z = \frac{\pi}{n}\left\{ 10\sin(\pi y_1) + \sum_{i=1}^{n-1} (y_i - 1)^2 \left[1 + 10\sin^2(\pi y_{i+1}) \right] + (y_n - 1)^2 \right\}$		
$y_i = 1 + \frac{x_1+1}{4}\, u(x_i, a, k, m) = \begin{cases} k(x_i - a)^m & x_i > a \\ 0 & -a < x_i < a \\ k(-x_i - a)^m & x_i < -a \end{cases}$		
$F_{13}(x) = 0.1z + \sum_{i=1}^{n} u(x_i, 5, 100, 4)$	[−50,50]	0
$z = \left\{ \sin^2(3\pi x_1) + \sum_{i=1}^{n} (x_i - 1)^2 \left[1 + \sin^2(3\pi x_i + 1) \right] + (x_n - 1)^2 \left[1 + \sin^2(2\pi x_n) \right] \right\}$		

Table 3 Fixed-dimension multimodal benchmark functions

Function	Variables	Range	$f_{\min}$
$F_{14}(x) = \left(\frac{1}{500} + \sum_{j=1}^{25} \frac{1}{j + \sum_{i=1}^{2} (x_1 - a_1)^6} \right)^{-1}$	2	[-65,65]	1
$F_{15}(x) = \sum_{i=1}^{11} \left[a_i - \frac{x_1 (b_i^2 + b_i x_2)}{b_i^2 + b_i x_3 + x_4} \right]^2$	4	[−5,5]	0.0003
$F_{16}(x) = 4x_1^2 - 2.1x_1^4 + \frac{1}{3}x_1^6 + x_1 x_2 - 4x_2^2 + 4x_2^4$	2	[−5,5]	−1.0316
$F_{17}(x) = \left(x_2 - \frac{5.1}{4\pi^2}x_1^2 + \frac{5}{\pi}x_1 - 6 \right)^2 + 10\left(1 - \frac{1}{8\pi}\right)\cos x_1 + 10$	2	[−5,5]	0.398
$F_{18}(x) = \left[1 + (x_1 + x_2 + 1)^2 \left(19 - 14x_1 + 3x_1^2 - 14x_2 + 6x_1 x_2 + 3x_2^2 \right) \right] \times z$	2	[−2,2]	3
$z = \left[30 + (2x_1 - 3x_2)^2 \times \left(18 - 32x_1 + 12x_1^2 + 48x_2 - 36x_1 x_2 + 27x_2^2 \right) \right]$			
$F_{19}(x) = -\sum_{i=1}^{4} c_i \exp\left(-\sum_{j=1}^{3} a_{ij} \left(x_j - p_{ij} \right)^2 \right)$	3	[1,3]	−3.86
$F_{20}(x) = -\sum_{i=1}^{4} c_i \exp\left(-\sum_{j=1}^{6} a_{ij} \left(x_j - p_{ij} \right)^2 \right)$	6	[0,1]	−3.32
$F_{21}(x) = -\sum_{i=1}^{5} \left[(X - a_i)(X - a_i)^T + c_i \right]^{-1}$	4	[0,10]	−10.1532
$F_{22}(x) = -\sum_{i=1}^{7} \left[(X - a_i)(X - a_i)^T + c_i \right]^{-1}$	4	[0,10]	−10.4028
$F_{23}(x) = -\sum_{i=1}^{10} \left[(X - a_i)(X - a_i)^T + c_i \right]^{-1}$	4	[0,10]	−10.5363

Table 4 CEC-C06 2019 benchmark functions" (Price et al. 2018; Yeh et al. 2019)

	Function	Dimension	Range	$f_{\min}$
F_{CEC1}	Storn's Chebyshev polynomial fitting problem	9	[−8192, 8192]	1
F_{CEC2}	Inverse hilbert matrix problem	16	[−16384, 16384]	1
F_{CEC3}	Lennard-Jones minimum energy cluster	18	[−4,4]	1
F_{CEC4}	Rastrigin function	10	[−100, 100]	1
F_{CEC5}	Griewank function	10	[−100, 100]	1
F_{CEC6}	Weierstrass function	10	[−100, 100]	1
F_{CEC7}	Modified schwefel function	10	[−100, 100]	1
F_{CEC8}	Expanded schaffer F6 function	10	[−100, 100]	1
F_{CEC9}	Happy cat function	10	[−100, 100]	1
F_{CEC10}	Ackley function	10	[−100, 100]	1

losses and to obtain better voltage profiles. In addition, management of charging and discharging periods of ESSs can be used efficiently for peak shaving purposes (Ahmadi et al. 2021). One of the approaches to improve the voltage profiles aims to minimize the sum of absolute difference between the voltage magnitudes of reference bus and the remaining feeder buses. Another approach reported in Ahmadi et al. (2019b) achieves the voltage profile improvement by minimizing the voltage magnitude differences of the neighboring buses. Moreover, different types of power and energy loss-based objective functions that are suitable for specific applications can be used. All the aforementioned planning problems are incorporated several constraints such as power balance equations and upper and lower limits of DG and ESS parameters.

The following subsections present the formulation of the objective function of the planning problem in smart grids.

4.3.1 Voltage profile improvement

We use two different voltage profile improvement formulations. The first one models the voltage profile improvement problem as minimization of the squared sum of the differences between the bus voltage magnitude of each connected bus;

$$f_1 = \sum_{i=1}^{N_T} \sum_{j=1}^{N_{BUS}} \left[\sum_{k} (V_j^i - V_k^i)^2 \right] \tag{19}$$

where N_T denotes the total hours of simulation, N_{BUS} is the number of busses in the feeder, and V_j^i is the bus voltage magnitude at bus j at hour i.

The second formulation is defined as the squared sum of the voltage magnitude differences between the reference bus and the remaining feeder busses;

$$f_2 = \sum_{i=1}^{N_T} \sum_{j=1}^{N_{BUS}} \left[(V_j^i - V_{ref})^2 \right] \tag{20}$$

Table 5 Emission intensities and cost of pollution gases

	SO_2	NO_x	CO_2	CO
Emission intensity (g/kWh)	6.48	2.88	623	0.1083
Environmental value ($/kg)	0.875	1.25	0.0041	0.145

where N_T denotes the total hours of the simulation period, N_{BUS} is the number of buses in the feeder, and V_j^i is the bus voltage magnitude at bus j at hour i. Reference voltage is shown by V_{ref}.

4.3.2 Total energy losses

Active power loss of the jth branch in the system at time i can be calculated as $Pl_j^i = (I_j^i)^2 \times R_j$, where, R_j is the resistance of the jth branch. Total energy losses along the simulation period can be expressed as follows:

$$f_3 = \sum_{i=1}^{N_T} \sum_{j=1}^{N_{br}} Pl_j^i \tag{21}$$

4.3.3 Emission costs of thermal power plants

In recent years, the global warming has been a major issue due to the continuous growth of greenhouse gas emissions from different sources. Greenhouse gases such as CO_2, CO, SO_2, and NO_x are mainly blamed for global warming and occupy a large volume of the total emissions. Atmospheric emissions costs of the grid mainly arise due to purchasing electricity from the thermal power plants. Emission intensities and environmental costs of those gases are shown in Table 5 (Liu et al. 2015). Annual emission cost of the thermal generating units in the main grid can be expressed as follows:

$$f_4 = \left(\sum_{j=1}^{N_g} K_j \times E_j \right) \sum_{i=1}^{8760} P_{MG_i} \tag{22}$$

where K_j and E_j are environmental value and emission intensity of jth generating unit, respectively. P_{MG_i} shows the active power generated by the ith thermal unit.

4.3.4 Problem constraints

The power balance constraints and other operational constraints are described as follows.

1. Power balance: generated power should be equal to the sum of the consumed one and the losses at each hour of the optimization period.

$$\begin{aligned} P_{\mathrm{MG}_i} + P_{\mathrm{DG}_i} + P_{\mathrm{ESSC/D}_i} - P_{\mathrm{load}_i} - P_{\mathrm{losses}_i} &= 0 \\ Q_{\mathrm{MG}_i} - Q_{\mathrm{load}_i} - Q_{\mathrm{losses}_i} &= 0 \\ i = 1, 2, \cdots, N_{\mathrm{T}} \end{aligned} \tag{23}$$

   where P_{MG} and Q_{MG} are the active and reactive power supplied from the main grid at the slack bus. P_{DG} is the total active power generated by DGs. P_{ESSD} and P_{ESSC} denote discharge and charge powers of ESS units, respectively. The active and reactive load and losses are represented by P_{load}, P_{losses}, Q_{load}, and Q_{losses}.
2. Generation constraints: the upper limit of DG units are assumed to be 1 MW due to governmental incentives provided for small scale DG units in Turkey. DG installation capacity at each bus except the slack bus cannot exceed 1 MW. On the other hand, the main grid supply is limited due to generation and load profiles at each hour.

$$P_{\mathrm{MG}_i} \leq P_{\mathrm{MG}_{max}} \tag{24}$$

$$Q_{\mathrm{MG}_i} \leq Q_{\mathrm{MG}_{max}} \tag{25}$$

$$P_{\mathrm{DG}} \leq P_{\mathrm{DG}_{max}} \tag{26}$$

3. ESS constraints: the upper limit for ESS energy sizes is set as 1 MWh, while their charging/discharging amounts are restricted at each time step, to limit the available energy (state of charge -SoC) of the units. Charging and discharging strategies are same for all ESS units at each time step to avoid power exchange between ESS units. The constraints of ESS units can be formulated as follows.

$$\mathrm{E}_{\mathrm{ESS}} \leq \mathrm{E}_{\mathrm{ESS}_{max}} \tag{27}$$

$$(P_{\mathrm{ESSC}_i}, P_{\mathrm{ESSD}_i}) \leq 1MW \tag{28}$$

$$0.2 * E_{\mathrm{ESS}} \leq SOC_{\mathrm{ESS}_i} \leq 0.8 * E_{\mathrm{ESS}} \tag{29}$$

4. Voltage violation problems are embedded in the objective function as penalty terms. Note that penalty at the final result will be zero if all voltage magnitudes are within the pre-specified limits.

$$P^i = K \times \begin{cases} (v_j^i - 0.95)^2, & \text{if } v_j^i < 0.95 \\ 0, & \text{if } 0.95 < v_j^i < 1.05 \\ (v_j^i - 1.05)^2, & \text{if } v_j^i > 1.05 \end{cases} \tag{30}$$

4.4 AGWO Implementation for smart grid problems

The framework of the proposed AGWO for determining the near-optimal size, site, and operation strategy of DG and ESS units is given in the following steps:

1. Provide input data including maximum number of DGs and ESSs, location and size restrictions, stopping criteria (maximum number of iterations and tolerance), number of search agents, maximum archive size, test system line data, scaled outputs of DGs, and load data.
2. Initialize solution candidates (initial DG locations, sizes and types, capacity and locations of ESSs, and ESSs charge and discharge variables for each hour) randomly within the feasible solution space.
3. Calculate the objective values for each search agent, performing the Forward–Backward Sweep (FBS) power flow (Eminoglu and Hocaoglu 2009) and update the α, β, and δ position variables.
4. Decide either using the ω position variables in the exploitation phase or generate the new position variables using (12).
5. Update the positions using the proposed AGWO position evaluation formulations.
6. Check the new solution boundaries and revise them with respect to the proposed approach, if they violate the limits.
7. Check stopping condition (either using the maximum iteration number or comparing the average of best solution distance to origin at the current iteration and predetermined number of iterations before) and repeat 3.

4.5 The parameters of the optimization algorithms

For all the algorithms and test functions, the population sizes are set to 30 and the remaining parameters are empirically determined as also indicated in Heidari and Pahlavani (2017); Geem et al. (2001). HS parameters are set as follows. The harmony memory consideration rate (HMCR) and pitch adjusting rate (PAR) are set to 0.9 and 0.1, respectively. We set the distance bandwidth (BW) to $0.02 \times (ub - lb)$ and the damping ratio to 0.95. In PSO, the parameters: c1 and c2 are the learning factors and set to 1.49. We set Inertia factor (IF)

Table 6 Results of unimodal and multimodal benchmark functions with 30 variables

F	AGWO		GWO		PSO		ALO		SSA		HS	
	Avg	Std	Avg	Std	Avg	Std	Avg	Std	Avg	Std	Avg	Std
F_1	**8.4E − 62**	2.3E−31	7.4E−59	1.2E−58	1.3E−8	2.2E−8	8.2E−6	7.3E−6	1.2E−8	2.4E−9	90.8	36.6
F_2	8.2E−32	1.4E−35	**8.7E − 35**	9.1E−35	7.3E−4	1.3E−3	28.3	43.6	0.96	1.2	1.3	0.4
F_3	**7.5E − 20**	2.1E−19	2.5E−15	8.1E−15	14.7	7.9	1510.2	1010.1	252.1	144.9	11299.9	4600.1
F_4	**1.4E − 15**	1.5E−11	2.1E−14	3.8E−14	0.58	0.14	12.5	4.0	7.2	3.5	15.2	1.7
F_5	**26.03**	0.58	27.2	0.76	60.9	51.4	115.1	200.2	140.9	344.1	4330.1	2700.0
F_6	1.6E−5	1.2E−5	0.71	0.38	**1.9E − 8**	6.0E−8	1.1E−5	9.5E−6	1.2E−8	2.9E−9	79.7	29.1
F_7	**2.7E − 4**	7.5E−5	8E−4	5.2E−4	6.6E−2	2.7E−2	0.1	3.8E−2	9.3E−2	4.1E−2	0.11	2.7E−2
F_8	−7360.7	453.8	−6019.1	997.2	−6170.8	1575.6	−5484.5	76.0	−7700.8˜	763.1	**−12521.0**	21.5
F_9	**0**	0	0.86	2.58	45.55	10.73	89.6	21.8	56.5	16.8	9.9	2.5
F_{10}	**1.1E − 14**	3.1E−15	1.6E−14	2.4E−15	2.5E−4	5.3E−4	2.11	1.2	2.2	0.8	3.3	0.4
F_{11}	**0**	0	2E−3	5.4E−3	6.9E−3	5.9E−3	9.3E−3	8.8E−3	1.1E−2	1.4E−2	1.8	0.3
F_{12}	**6.4E − 3**	7.0E−3	4E−2	2.4E−2	3.5E−3	1.9E−2	10.9	3.8	4.8	3.1	1.7	0.6
F_{13}	**9.1E − 2**	0.11	0.52	0.23	3.3E−3	5.1E−3	3.17	11.1	4.3	10.4	14.0	3.5

to 0.72 with a damping ratio of 0.9 over the iterations. Note that the GWO, SSA, and ALO are parameter-free methods and we set the number of function evaluations equal to each other by adjusting the number of maximum iterations. We run the algorithms 50 times with the same conditions using a PC with 16GB RAM, intel core i7-7700 3.6GHz processor configuration using MATLAB version 2018b.

5 Results and discussion

5.1 Simulation analysis for classical optimization test functions

Simulation results of 50 trials for each test function are recorded together with their averages and standard deviations. We show the best mean values with the bold characters in the tables related to simulation results. From our experiments, we determined optimal b_1 and b_2 parameters from Eq. (11) as 0.5 and 0.4, respectively. The simulation results are shown in Tables 6, 7, 8 and 9 for unimodal benchmark functions and multimodal benchmark functions. The results show that for 10 and 9 out of 13 unimodal and multimodal benchmark functions using 30 variables and 60 variables, respectively, AGWO finds better near optimal values. For F2, GWO finds better average value of near optimal value, for F6, PSO is better and for F8, HS finds the best value of the objective function using 30 variables. In the case of 60 variables, PSO finds the best result for F6, F12 and F3, HS finds the best result for F8. When the case of fixed dimension multimodal benchmark functions is considered as given in Table 10 and 11, it is observed that the best numerical results are again obtained using AGWO. For F15, F20, F21, F22 and F23 AGWO provides the best results. For only F14, SSA finds the best result. For the remaining cases, all methods are able to find the best objective function values. From these results, it is obvious that AGWO, regardless of the variable size, can find better solutions than other tested algorithms (Tables 7, 8, 9, 10, 11, 12 and 13).

5.2 Simulation analysis for CEC-C06 2019 benchmark test functions

We used the same parameter sets for CEC Benchmark Test Functions as in the previous test simulations. The average and standard deviation results of 50 individual runs of the algorithms are reported in Table 12 and 13. As shown in Table 12 and 13, AGWO result shows better results than other algorithms for all the CEC functions except F_{CEC2} and F_{CEC3} functions. It can be observed that except PSO, all other methods are able to find the same minimum value for F_{CEC2}, AGWO giving the smallest standard deviation. For F_{CEC3}, all methods find the same minimum value; again AGWO produces the smallest standard deviation.

5.3 Simulation analysis for smart grid planning problems

In order to assess the efficiency of the proposed AGWO algorithm to solve allocation problem of DGs and ESSs, four case studies have been considered. These cases are:

1. Voltage profile improvement using objective function f_1.
2. Voltage profile improvement using objective function f_2.
3. Minimization of energy losses using objective function f_3.

Table 7 Execution times for unimodal and multimodal benchmark functions with 30 variables

F	AGWO		GWO		PSO		ALO		SSA		HS	
	Avg	Std	Avg	Std	Avg	Std	Avg	Std	Avg	Std	Avg	Std
F_1	0.26	0.01	0.26	0.01	0.10	0.01	35.23	0.33	0.17	0.01	0.19	0.01
F_2	0.27	5E−3	0.27	5E−3	0.10	0.01	35.80	0.42	0.18	0.01	0.20	0.01
F_3	0.57	0.02	0.58	0.03	0.39	0.03	36.32	0.12	0.49	0.03	0.51	0.03
F_4	0.26	0.01	0.27	0.01	0.10	0.01	35.98	0.17	0.18	0.01	0.19	0.01
F_5	0.32	0.01	0.33	0.01	0.14	0.01	36.17	0.22	0.24	0.01	0.25	0.01
F_6	0.26	0.01	0.27	0.01	0.10	0.01	36.15	0.06	0.18	0.01	0.20	0.01
F_7	0.42	0.01	0.43	0.01	0.25	0.01	36.17	0.20	0.34	0.01	0.36	0.01
F_8	0.31	0.01	0.32	0.01	0.15	0.01	36.01	0.17	0.22	0.01	0.24	0.01
F_9	0.27	4E−3	0.28	5E−3	0.12	4E−3	36.11	0.11	0.20	5E−3	0.21	0.01
F_{10}	0.28	0.01	0.29	0.01	0.13	0.01	36.01	0.18	0.21	0.01	0.23	0.01
F_{11}	0.33	0.01	0.34	0.01	0.17	0.01	35.97	0.27	0.26	0.01	0.28	0.01
F_{12}	0.73	0.01	0.73	0.01	0.55	0.01	36.31	1.28	0.64	0.01	0.66	0.01
F_{13}	0.71	0.01	0.72	0.01	0.54	0.01	35.48	0.13	0.63	5E−3	0.65	5E−3

Table 8 Results of unimodal and multimodal benchmark functions with 60 variables

F	AGWO		GWO		PSO		ALO		SSA		HS	
	Avg	Std	Avg	Std	Avg	Std	Avg	Std	Avg	Std	Avg	Std
F_1	**4.8E − 130**	1.9E−129	2.3E−125	8.4E−125	1.7E−7	3.9E−7	1.1E−6	6.3E−7	0.58	0.13	2110	241.5
F_2	**2.5E − 75**	6.5E−75	5.1E−74	5.2E−74	1.6E−3	2.3E−3	117.9	109.6	23.9	60.1	14.9	1.4
F_3	**1.0E − 29**	2.8E−29	5.6E−25	2.7E−20	317.2	77.3	3490.1	1070.2	677.9	190.1	88500	12E3
F_4	**8.0E − 28**	1.9E−28	1.5E−25	3.3E−25	1.97	0.22	19.4	4.55	3.99	1.18	31.4	2.08
F_5	**55.2**	0.62	57.1	0.98	110.0	40.6	224.2	352.9	345.0	588.0	4.7E5	99E3
F_6	1.33	0.98	3.04	0.79	**1.6E − 7**	3.8E−7	8.7E−7	3.1E−7	0.56	0.13	2190.0	300.0
F_7	**1.8E − 4**	5.9E−5	4.3E−4	1.8E−4	0.22	6.8E−2	9.7E−2	2.7E−2	4.5E−2	1.3E−2	0.80	0.17
F_8	−14347.1	54.98	−10944.2	1279.5	−12824.1	2260.5	−11344.1	2606.0	−15343.0	879.7	**−24174.0**	207.1
F_9	**0**	0	7.6E−15	2.9E−14	135.8	24.7	171.5	33.1	274.1	58.2	60.8	5.4
F_{10}	**1.1E − 14**	3.0E−15	1.5E−14	2.1E−15	0.26	0.59	2.66	1.03	1.64	0.51	7.9	0.46
F_{11}	**0**	0	9.4E−4	3.9E−3	1.7E−3	3.2E−3	3.9E−3	6.5E−3	0.59	7.5E−2	19.8	2.3
F_{12}	0.05	0.03	0.11	0.04	**6.9E − 3**	0.02	10.79	2.79	3.00	0.94	346.5	579.4
F_{13}	1.74	0.38	2.43	0.35	**0.02**	0.05	14.56	25.05	0.26	0.33	1.4E5	67020

4. Minimization of hybrid objective function F that is a linear combination of f_1, f_3, and f_4. We define F function by summing and taking the average of the normalized sums of each function as follows:

$$F = \frac{\frac{f_1}{f_1^{base}} + \frac{f_3}{f_3^{base}} + \frac{f_4}{f_4^{base}}}{3} \tag{31}$$

5.3.1 Line and load model characteristic of DNs

The distribution networks used in this study are 33-bus and 141-bus radial distribution systems. System data are taken from (Baran and Wu April 1989; Khodr et al. 2008). The 33-bus system peak load is 3.715 MW and corresponding power losses at this level is 201.9kW. Similarly, peak load and corresponding power losses for 141-bus test system are 11.890 MW and 628.2 kW, respectively. Daily load curves of a representative Turkish medium voltage distribution feeder (Guner and Ozdemir 2020), industrial, residential, and commercial (Yammani et al. 2016) model load curves have been adopted for the study. Normalized load patterns used in the study are shown in Fig. 4. In this context, active and reactive loads at each hour of the simulation period are determined by scaling the load variation curve with the peak load of (Baran and Wu April 1989) and (Khodr et al. 2008). Note that the peaks and the valleys in the curve are the critical periods for prospective under-voltage and over-voltage problems, respectively.

Table 9 Execution times for unimodal and multimodal benchmark functions with 60 variables

F	AGWO		GWO		PSO		ALO		SSA		HS	
	Avg	Std	Avg	Std	Avg	Std	Avg	Std	Avg	Std	Avg	Std
F_1	0.44	0.01	0.46	0.02	0.16	0.02	69.98	0.20	0.28	0.01	0.31	0.01
F_2	0.45	0.76	0.48	0.38	0.17	5E−3	69.80	0.14	0.29	4E−3	0.32	4E−3
F_3	1.04	0.03	1.06	0.02	0.74	0.02	70.47	0.22	0.88	0.02	0.91	0.02
F_4	0.42	0.01	0.46	5E−3	0.16	0.01	69.64	0.09	0.28	4E−3	0.32	0.01
F_5	0.50	0.01	0.52	0.01	0.20	0.01	69.69	0.10	0.33	4E−3	0.37	5E−3
F_6	0.44	5E−3	0.46	3E−3	0.16	0.01	69.63	0.09	0.28	0.56	0.31	5E−3
F_7	0.71	0.01	0.74	4E−3	0.42	0.01	69.93	0.12	0.55	4E−3	0.59	5E−3
F_8	0.51	0.01	0.53	5E−3	0.24	0.01	69.70	0.33	0.34	5E−3	0.38	0.01
F_9	0.46	0.01	0.48	5E−3	0.21	5E−3	69.59	0.12	0.32	4E−3	0.35	0.01
F_{10}	0.47	0.01	0.49	0.01	0.21	0.01	69.64	0.12	0.33	0.01	0.38	0.01
F_{11}	1.54	0.05	1.71	0.07	0.80	0.04	756.43	12.00	1.18	0.03	1.36	0.03
F_{12}	3.40	0.03	3.65	0.05	2.65	0.02	741.86	2.20	3.01	0.01	3.19	0.01
F_{13}	3.40	0.03	3.64	0.03	2.66	0.02	740.86	5.29	3.04	0.02	3.22	0.02

Table 10 Results of fixed-dimension multimodal benchmark functions

F	AGWO		GWO		PSO		ALO		SSA		HS	
	Avg	Std	Avg	Std	Avg	Std	Avg	Std	Avg	Std	Avg	Std
F_{14}	2.18	2.5	3.86	4.3	2.54	2.2	1.49	1.03	**1.00**	8E−12	3.43	2.7
F_{15}	**3.1E − 4**	8.9E−7	5E−3	8.6E−3	8E−4	2.2E−4	1.4E−3	3.6E−3	3.3E−3	6.8E−3	9E−4	2.6E−4
F_{16}	−1.03	9.5E−12	−1.03	7.1E−9	−1.03	6.6E−16	−1.03	5.9E−14	−1.03	9.1E−8	−1.03	6.6E−16
F_{17}	0.4	3.6E−7	0.40	2.5E−5	0.40	0	0.40	5.5E−14	0.40	1.6E−7	0.40	0
F_{18}	3.0	2.6E−6	3.00	1.1E−5	3.00	7.6E−16	3.00	2.4E−13	3.00	5.6E−7	3.00	1.7E−15
F_{19}	−3.86	3.8E−4	−3.86	2.4E−3	−3.86	2.7E−15	−3.86	2.1E−4	−3.86	9.3E−7	−3.86	2.7E−15
F_{20}	**−3.29**	5.5E−2	−3.27	7E−2	−3.28	5.8E−2	−3.27	5.9E−2	−3.25	6E−2	−3.28	5.8E−2
F_{21}	**−10.2**	2.1E−4	−9.9	0.92	−7.3	3.40	−6.88	2.97	−6.95	2.95	−7.8	3.07
F_{22}	**−10.4**	1.8E−4	**−10.4**	2.3E−4	−8.9	2.63	−6.9	3.24	−8.0	3.11	−9.6	2.06
F_{23}	**−10.5**	1.7E−4	**−10.5**	2.7E−4	−9.8	1.99	−8.0	3.22	−9.1	2.68	−10.0	1.64

Table 11 Execution times for fixed-dimension multimodal benchmark functions

F	AGWO		GWO		PSO		ALO		SSA		HS	
	Avg	Std	Avg	Std	Avg	Std	Avg	Std	Avg	Std	Avg	Std
F_{14}	1.02	0.05	1.01	0.05	0.93	0.05	3.94	0.07	1.02	0.05	1.01	0.05
F_{15}	0.11	6E−3	0.10	5E−3	0.05	4E−3	5.55	0.05	0.10	5E−3	0.10	5E−3
F_{16}	0.09	1E−3	0.08	3E−3	0.04	1E−3	3.00	0.03	0.09	1E−3	0.08	1E−3
F_{17}	0.08	0.01	0.07	0.01	0.04	0.01	2.98	0.03	0.08	0.01	0.07	0.01
F_{18}	0.08	0.01	0.07	0.01	0.03	0.01	2.99	0.03	0.07	0.01	0.07	0.01
F_{19}	0.12	5E−4	0.10	3E−3	0.06	4E−4	4.47	0.01	0.11	4E−4	0.11	5E−4
F_{20}	0.13	4E−3	0.13	0.01	0.07	2E−3	8.13	0.10	0.12	2E−3	0.12	2E−3
F_{21}	0.13	2E−3	0.12	4E−3	0.07	2E−3	5.54	0.02	0.12	3E−3	0.12	2E−3
F_{22}	0.15	1E−3	0.14	4E−3	0.09	1E−3	5.57	0.02	0.14	1E−3	0.13	1E−3
F_{23}	0.17	4E−3	0.16	4E−3	0.11	3E−3	5.62	0.08	0.16	3E−3	0.15	2E−3

5.3.2 Modeling PV and WT configurations

The study uses 10-year wind speed and solar radiation data of a specific location in Turkey—by specifying the latitude and longitude of Karaman region (Pfenninger and Staffell 2016; Staffell and Pfenninger 2016)—to estimate DG outputs. The time sequence characteristic of each DG type is illustrated in Fig. 5. We assume the same output patterns for all WTs

Table 12 Results of CEC-C06 2019 benchmark functions

F	AGWO		GWO		PSO		ALO		SSA		HS	
	Avg	Std	Avg	Std	Avg	Std	Avg	Std	Avg	Std	Avg	Std
F_{CEC1}	**4.0E+4**	1.2E+3	8.8E+7	1.5E+8	1.1E+12	2.7E+12	5.5E+9	4.2E+9	1.0E+8	2.0E+8	1.1E+8	2.2E+8
F_{CEC2}	17.3	1.0E−4	17.3	1.6E−4	10326.7	3.7E+3	17.3	2.0E−4	17.3	1.6E−4	17.3	1.9E−4
F_{CEC3}	12.7	3.6E−15	12.7	3.0E−6	12.7	3.7E−15	12.7	4.7E−15	12.7	1.4E−6	12.7	5.73E−7
F_{CEC4}	**5.0**	9.1E−16	266.8	9.0E+2	12.0	3.6	23.3	8.6	272.3	8.9E+2	199.6	3.99E+2
F_{CEC5}	**1.0**	2.3E−16	1.3	2.3E−1	1.1	9.3E−2	1.2	6.7E−2	1.4	2.6E−1	1.4	2.4E−1
F_{CEC6}	**2.0**	1.0	11.2	7.5E−1	9.5	1.0	4.9	1.7	11.1	6.8E−1	10.8	1.0
F_{CEC7}	**6.3**	8.5	40.8	1.3E+2	170.8	1.0E+2	379.4	2.6E+2	625.3	2.9E+2	505.6	3.5E+2
F_{CEC8}	**1.4**	7.7E−1	4.7	1.0	5.3	5.4E−1	5.4	7.7E−1	4.2	1.3	4.7	9.0E−1
F_{CEC9}	**2.3**	3.6E−5	4.7	9.7E−1	2.4	6.8E−3	2.4	3.2E−2	4.3	6.1E−1	4.2	5.8E−1
F_{CEC10}	**10.1**	3.5	19.9	2.2	20.1	1.3E−1	20.0	5.0E−2	20.5	7.2E−2	20.4	9.7E−2

Table 13 Execution times for CEC-C06 2019 benchmark functions

F	AGWO		GWO		PSO		ALO		SSA		HS	
	Avg	Std	Avg	Std	Avg	Std	Avg	Std	Avg	Std	Avg	Std
F_{CEC1}	7.58	0.06	7.58	0.09	7.50	0.06	19.29	0.13	7.56	0.06	7.55	0.06
F_{CEC2}	0.17	5E−3	0.17	0.01	0.07	0.01	19.72	0.18	0.13	5E−3	0.13	0.01
F_{CEC3}	0.25	3E−3	0.25	0.01	0.14	1E−3	22.79	0.15	0.20	2E−3	0.20	2E−3
F_{CEC4}	0.16	3E−4	0.15	3E−3	0.07	1E−3	13.07	0.04	0.13	1E−3	0.13	1E−3
F_{CEC5}	0.17	5E−3	0.16	0.01	0.08	5E−3	13.01	0.06	0.14	5E−3	0.14	0.01
F_{CEC6}	2.60	0.02	2.60	0.03	2.51	0.02	15.51	0.10	2.59	0.02	2.58	0.02
F_{CEC7}	0.17	0.01	0.17	0.01	0.09	0.01	13.06	0.11	0.15	0.01	0.14	0.01
F_{CEC8}	0.17	0.01	0.17	0.01	0.08	0.01	13.01	0.12	0.15	0.01	0.14	0.01
F_{CEC9}	0.15	0.01	0.15	0.01	0.07	0.01	13.01	0.10	0.13	0.01	0.12	0.01
F_{CEC10}	0.17	4E−3	0.17	5E−3	0.09	4E−3	13.14	0.05	0.15	4E−3	0.14	4E−3

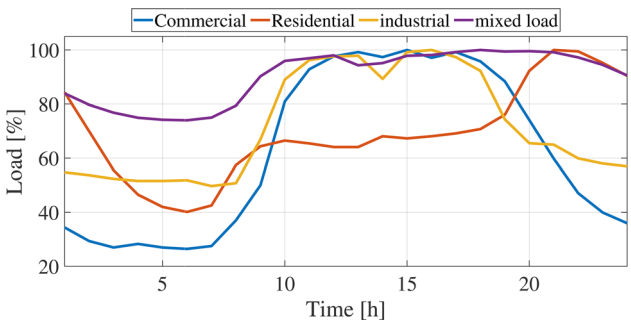

Fig. 4 Scaled load curves

(with an average 35% total mean capacity factor) and PV generations (with an average 35% total mean capacity factor) as they will be allocated at the same territory.

We determined the simulation parameters by performing several runs by using high number iterations as follows. The maximum number of iterations and the number of search agents are set 2000, and 30, respectively. The maximum DG and ESS unit numbers are set as 10. We use tolerance value of 10^{-5} for stopping where the algorithm compares the best objective value in the current iteration with that of 50 iterations before.

5.3.3 33-bus test system

The algorithms found the optimal DG and ESS units number to allocating in the proposed system. The maximum number of iteration and tolerance parameters found empirically. The number of variables is 300. From these, we dedicate 30 of them to determine DG unit sizes, sites and types, and 20 of them to determine the capacities and the locations of ESSs. The remaining variables are used to find the optimal SoC of ESS units. We performed 20 runs and calculated the average and standard deviations of the resulting outputs.

We designed f_1 to improve the voltage profile and, thus, to reduce the power losses. Since the objective function tries to bring the voltage magnitudes of connected busses to be as close as possible, it can reduce the losses. The same objective can also be formulated as f_2 objective function, which aims to bring all the voltage magnitudes near to the reference voltage magnitude. The f_3 function tries to reduce the system energy losses along the optimization period, and finally, the f_4 is

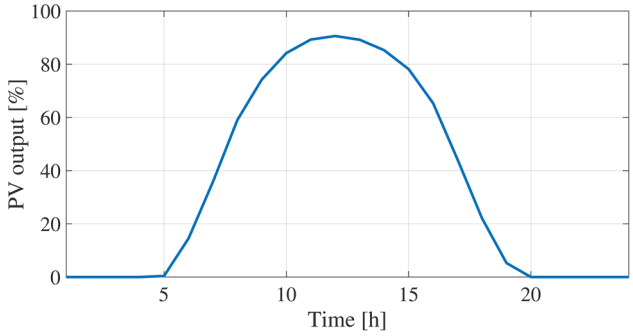

(a) PV output.

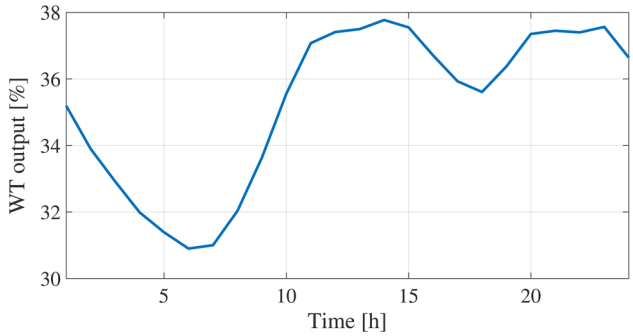

(b) WT output.

Fig. 5 Scaled DG outputs

Table 14 Base case objective function values in 33-bus system

	f_1^{base}	f_2^{base}	f_3^{base}	F^{base}
Commercial	0.4068	1.3004	2.2576	1
Residential	0.1587	1.3703	2.6065	1
Industrial	0.0405	1.5011	3.9385	1
Mixed	0.1917	2.2696	2.3802	1

designed to minimize the emission cost of thermal units. F is a linear combination of scaled marginal objective functions. Objective function values are shown in Table 14 for the base case conditions, where there weren't any DG and ESS units.

Simulation results for different load curve characteristics (LCC) are shown in Table 15 where best result (BR) is the best value obtained by the proposed algorithm. The results show that AGWO finds the best (minimum) average values for each scenario and LCCs, besides f_3 with commercial LCC. In fact, the difference between AGWO result and the minimum one at this exceptional case is too small. Moreover, AGWO provides more consistent results as the standard deviations for AGWO are less than the ones obtained with the other methods.

For a detailed illustration of the results, we chose objective function F with the mixed LCC, function where the BR was found as 0.28021 by the AGWO algorithm. The convergence characteristics obtained for each algorithm are given in Fig. 6. The figure shows that AGWO shows better performance and higher speed to find the near-optimal minimum compared to the GWO and PSO algorithms. The best AGWO solution corresponding to a BR value of 0.28021 finds 10 DG units and 3 ESS units with the sizes and locations given in Table 16. Figure 7 shows the improvement in the voltage profiles for this solution compared to the base case without installation of DG and ESS units. The results show that all the voltage magnitudes less than $0.95pu$ are brought back to feasible regions (between 0.95 and $1.05pu$). For example, minimum bus voltage magnitude value, which was 0.9134 pu at bus 18 for the base case operating condition, is upgraded to 0.9714 pu with this near-optimal solution. In the figure, each color shows the voltage profile of specific time for sample of load curve.

The total energy losses of 3.938 MWh for the base case condition are decreased to 1.295 MWh for the near-optimal solution. The active power losses at each feeder branch are shown in Fig. 8 for each simulation time. As shown in the figures, the losses reduce by 60% compared to the base case values. For the peak load hour (6 PM), the base case power losses are $201.88kW$, and for the near-optimal case, it decreases to 66 kW. We show the state of charge (SoC) for three ESS units in Fig. 9. The units are allowed to charge and discharge between 20 to 80% of capacity size. The results show that ESS units charge one time a day and discharge the energy stored one times per day. Moreover, ESS units are charged during the off-peak load hours and the stored energy is discharged along the peak load hours.

Final component of F, f_4, denotes the emission cost of the thermal units in the main grid. The aforementioned near-optimal solution reduces the greenhouse gas emissions of base case by 35.4%.

5.3.4 141-bus test system

The same simulations are performed for the same study cases in the 141-bus system. After experimenting several runs using a high number of iterations, the problem parameters are determined as follows. We use 5000 as the maximum number of iterations and set as the search agents population size. The number of maximum DGs and ESSs units is set as 10. The tolerance is set to 10^{-5}. We compare the best objective value of the current iteration to that of the one of 100 iterations before and determine whether the algorithm stops or continues accordingly.

Similar to 33 Bus Case, each simulation is performed 20 times, and the average and standard deviations are calculated and recorded.

Objective function values are illustrated in Table 17 for the base case conditions, where there weren't any DG and ESS units. The results for different LCCs are shown in Table 18 where BR represents the best near optimal objective function

Table 15 Results of objective functions for different LCC

Objective	LCC	AGWO		GWO		PSO		BR
		Ave	Std	Ave	Std	Ave	Std	
f_1	Commercial	**0.086513**	0.000647	0.086892	0.002064	0.094234	0.005508	0.08605
	Residential	**0.096443**	0.001388	0.100313	0.004464	0.123866	0.022477	0.09546
	Industrial	**0.029317**	0.001355	0.029967	0.002218	0.035939	0.001552	0.02835
	Mixed	**0.007923**	0.000417	0.009485	0.000745	0.014211	0.000911	0.00762
f_2	Commercial	**0.099003**	0.000462	0.106772	0.003601	0.133965	0.035772	0.09932
	Residential	**0.054963**	0.003774	0.061157	0.004843	0.196408	0.01522	0.05229
	Industrial	**0.042475**	0.001309	0.052259	0.008113	0.13947	0.046345	0.04154
	Mixed	**0.084298**	0.013698	0.091001	0.000846	0.360208	0.094391	0.07461
f_3	Commercial	0.880226	0.008648	**0.871937**	0.013226	0.937132	0.029113	0.86371
	Residential	**0.839561**	0.006448	0.842836	0.007351	1.063573	0.123761	0.83097
	Industrial	**0.912511**	0.014152	0.917371	0.015351	0.976617	0.09609	0.89998
	Mixed	**1.324694**	0.037517	1.362888	0.010124	1.716609	0.216865	1.28255
F	Commercial	**0.309308**	0.006564	0.314048	0.006753	0.406764	0.022163	0.29975
	Residential	**0.446737**	0.013033	0.446829	0.018986	0.559838	0.062712	0.43331
	Industrial	**0.277596**	0.004028	0.286145	0.004703	0.410216	0.042562	0.27216
	Mixed	**0.285511**	0.005826	0.292102	0.008464	0.422731	0.051966	0.28021

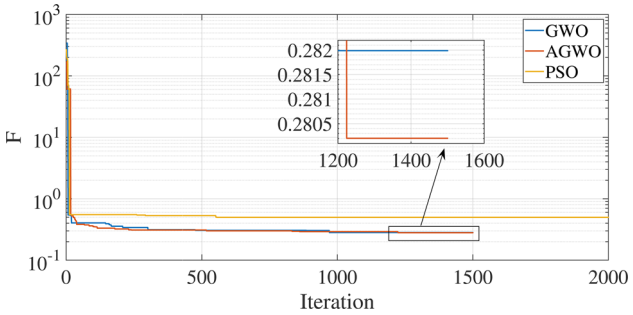

Fig. 6 Convergence characteristics of the three methods for objective function F

value calculated from proposed algorithm. The simulation results show that AGWO obtains better near-optimal minimum values compared to other algorithms besides two cases, namely f_2 under residential load condition and f_3 under mixed load condition. The results show that the proposed algorithm can reduce the energy losses for commercial, residential, industrial, and mixed LCC by 48.7%, 48.7%, 48.4%, and 42.2%,

For a detailed analysis, AGWO results are given for the representative objective function F with the mixed LCC, where the global minimum value was found to be 0.36624. The convergence curves given in Fig. 10 show that AGWO and GWO converge before the maximum number of iterations. Both methods converged at around 1500 iterations. AGWO finds 10 DG units and 5 ESS units. The locations, sizes and types of DGs and the locations, capacities and maximum powers of ESS units determined using AGWO are given in Table 19. Figure 11 shows the improvement in the system voltage profiles for this solution bringing the busses voltage magnitude between the 0.95 and 1.05pu. The minimum voltage in the base case was 0.9282pu, and it is improved to 0.9515pu in the near-optimal case.

The total energy losses in the base case was 12.275MWh. It is reduced to 7.085MWh for the obtained solution. The active power losses for each time of simulation and branches

Table 16 Optimum DG and ESS parameters obtained by AGWO for F under mixed LCC

DG						ESS		
Location	Size [kW]	Type	Location	Size [kW]	Type	Location	Capacity [kWh]	Max. power
5	960	WT	33	970	WT	22	300	23
18	940	WT	23	900	WT	17	840	65
32	950	WT	21	730	WT	14	360	27
25	880	WT	9	940	WT			
10	600	WT	6	850	WT			

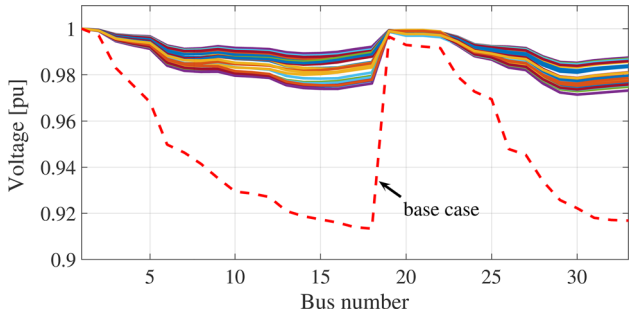

Fig. 7 33-bus system voltage profile

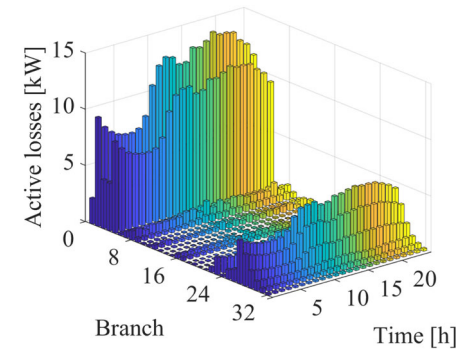

(a) Losses in the optimal case.

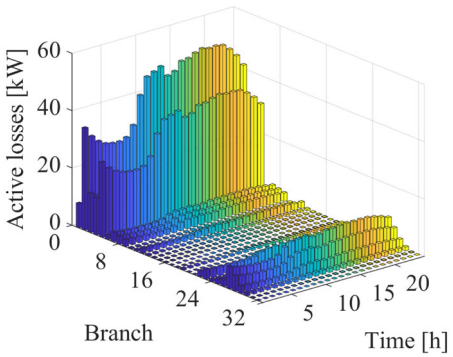

(b) Losses in the base case.

Fig. 8 Comparing losses in the optimal case and base case

are shown in Fig. 12. As shown in the figures, the power losses of the branches reduced up to 40% of the branch losses of the base case. For the peak load hour (6 PM), the base case's power losses was 628.2362kW, and for the optimal case, it was 380.6348kW. The SoC of ESSs illustrated in Fig. 13 shows that ESSs units charge in the off-peak load hours and discharge the stored energy in the peak load hours. Reduction in the emission cost of the thermal power plants was one of the aims in the F objective function. The optimal case found by the AGWO compared to the 141-bus system's base case reduced greenhouse gases by 69.9%.

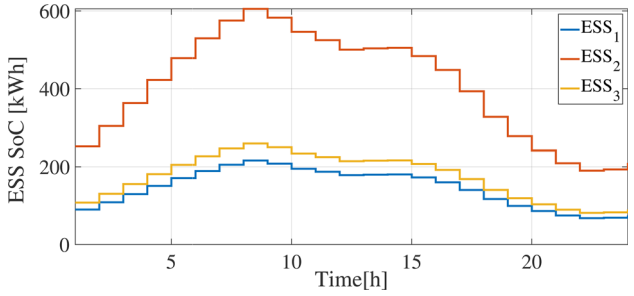

Fig. 9 SoC of ESS units

Table 17 Base case objective function values in 69-bus system

	f_1^{base}	f_2^{base}	f_3^{base}	F^{base}
Commercial	1.43591	4.2273	7.04313	1
Residential	0.58088	4.4657	7.4387	1
Industrial	0.12652	4.8853	8.13858	1
Mixed	0.50221	7.3668	12.27544	1

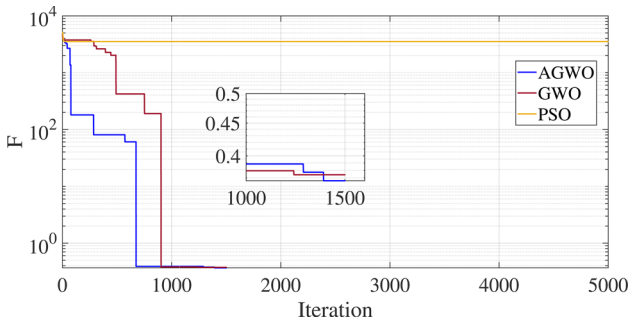

Fig. 10 Convergence characteristics of the three methods for objective function F in 141-bus test system

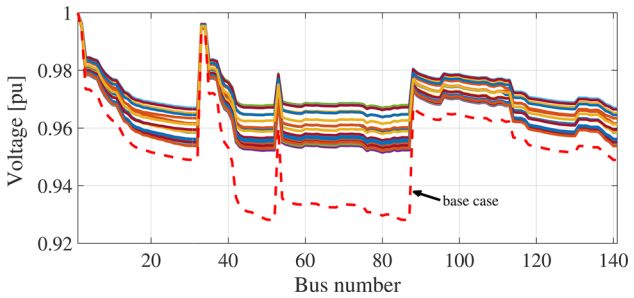

Fig. 11 141-bus system voltage profiles

6 Conclusions

This paper proposes an advanced version of the grey wolf optimizer algorithm termed as AGWO. Three modifications to GWO have been proposed, making it competitive with the other popular techniques. First, AGWO applies a dynamic

Table 18 Results of objective functions for different LCC

Objective	LCC	AGWO		GWO		PSO		BR
		Ave	Std	Ave	Std	Ave	Std	
f_1	Commercial	**0.405681**	0.004992	0.409233	0.006465	0.475545	0.037978	0.40051
	Residential	**0.454449**	0.005439	0.458711	0.006252	0.49597	0.021822	0.44692
	industrial	**0.135551**	0.002301	0.136027	0.001933	0.157953	0.010911	0.13271
	Mixed	**0.065364**	0.002653	0.065484	0.001288	0.090291	0.014376	0.06299
f_2	Commercial	**1.930609**	0.071012	1.972959	0.098465	2.595152	0.116991	1.86249
	Residential	2.217417	0.070692	**2.178377**	0.023719	2.866389	0.144293	2.15739
	Industrial	**2.329482**	0.107938	2.348665	0.066355	2.973097	0.121406	2.25667
	Mixed	**4.244081**	0.002081	4.325088	0.196928	5.801228	0.423166	4.24192
f_3	Commercial	**3.733583**	0.142794	3.80337	0.099378	84.33481	36.19676	3.61201
	Residential	**3.853046**	0.043372	8.926685	8.218557	142.9488	14.12767	3.81021
	Industrial	**4.236118**	0.051625	4.244826	0.115023	81.80521	14.03529	4.19504
	Mixed	9.038732	3.040671	**8.227236**	1.766291	397.2596	31.89096	7.08511
F	Commercial	**0.336332**	0.016139	0.363451	0.027395	1178.355	86.43253	0.31557
	Residential	**0.569128**	0.048371	0.570311	0.057963	1672.727	268.7774	0.50025
	Industrial	**0.255722**	0.007869	0.269666	0.012381	424.3396	259.8641	0.24261
	Mixed	**0.374421**	0.000252	0.411041	0.071298	3910.885	217.3359	0.36624

Table 19 Optimum DG and ESS parameters for 141-bus test system obtained by AGWO for F under mixed LCC

DG						ESS		
Location	Size [kW]	Type	Location	Size [kW]	Type	Location	Capacity [kWh]	Max. power [kW]
72	810	WT	75	420	WT	41	610	47
85	880	WT	64	660	WT	15	570	44
87	880	WT	51	750	WT	58	880	68
66	890	WT	69	980	WT	13	300	23
86	920	WT	46	930	WT	49	600	46

method to evaluate the search agent positions either in the exploitation or in the exploration phase. Second, AGWO uses a new formulation for evaluating the search agent position. It also checks the boundaries of the evaluated search agent position using a mirroring distance. These modifications improve the method helping to avoid early convergence and improve the exploration of the GWO algorithm. The performance of the AGWO has been evaluated by solving different classical benchmark test functions, CEC-C06 2019 functions and comparing the results to those obtained with the GWO, PSO, ALO, SSA, and HS algorithms. The experimental results of unimodal and multimodal functions show the better performance of AGWO even in higher dimensions.

AGWO does not require any sophisticated operators. Moreover it does not require complicated mathematical operations and various parameters. Thus, it is not expensive in terms of runtime and memory. This feature of AGWO makes it more adaptable to be used in several optimization problems. The numerical results obtained with AGWO show that the algorithm is suitable to be implemented in high dimensions and complex problems.

Moreover, this study solved a planning problem in smart grids to determine the optimal number, location of DGs and their types (WT and/or PV), and the charge/discharge amount of ESSs both on 33- and 141-bus test systems considering different load behaviors. The problem is solved by taking into different objective formulations, and the numerical results are compared to those of PSO and GWO. From the numerical results, we observe that smart grid optimization problem was solved with better voltage profiles, less losses, and less emission costs compared to the ones obtained with GWO and PSO. In future, we are planning to improve the algorithm so that multi-objective problems may be solved as well.

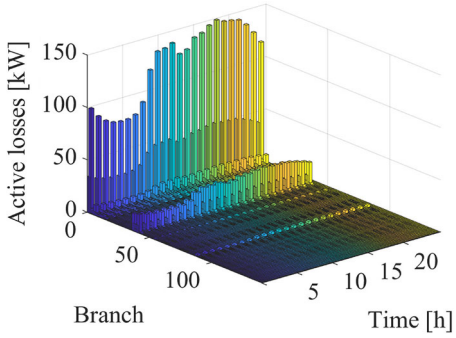

(a) Losses in the optimal case.

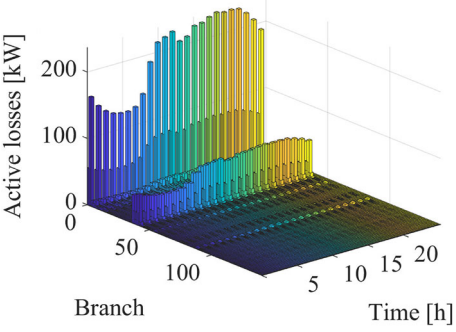

(b) Losses in the base case.

Fig. 12 Comparison of losses of the optimal and base cases

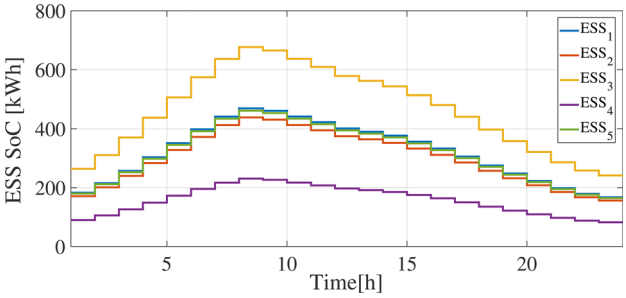

Fig. 13 SoC of ESS units: 141-bus test system

Acknowledgements This research is funded as a part of "117E773 Advanced Evolutionary Computation for Smart Grid and Smart Community" project under the framework of 1001 Project organized by "The Scientific and Technological Research Council of Turkey TUBITAK".

Author Contributions Bahman Ahmadi has made literature review, worked on software development, prepared the original draft, and visualized the simulation results. Soheil Younesi contributed to literature review and helped on preparing the draft. Oguzhan Ceylan contributed to methodology, data curation, review and editing, and formal analysis. Aydogan Ozdemir contributed to conceptualization and validation. He supervised the study and administered the project.

Funding This research is funded as a part of "117E773 Advanced Evolutionary Computation for Smart Grid and Smart Community" project under the framework of 1001 Project organized by "The Scientific and Technological Research Council of Turkey TUBITAK".

Data availability Not Applicable

Code availability The datasets generated during and/or analyzed during the current study are available from the corresponding author on reasonable request.

Declarations

Conflict of interest The authors have no conflicts of interest to declare that are relevant to the content of this article. Availability of data and material (data transparency).

References

Abdullah JM, Ahmed T (2019) Fitness dependent optimizer: inspired by the bee swarming reproductive process. IEEE Access 7:43473–43486

Abualigah L, Diabat A, Mirjalili S, Elaziz MA, Gandomi AH (2021) The arithmetic optimization algorithm. Comput Methods Appl Mech Eng 376:113609

Abualigah L, Yousri D, Elaziz MA, Ewees AA, Al-qaness MAA, Gandomi AH (2021) Aquila optimizer: a novel meta-heuristic optimization algorithm. Comput Indust Eng 157:107250

Ahmadi B, Ceylan O, Ozdemir A (2021) A multi-objective optimization evaluation framework for integration of distributed energy resources. J Energy Storage 41:103005

Ahmadi B, Ceylan O, Ozdemir A (2021) Distributed energy resource allocation using multi-objective grasshopper optimization algorithm. Electric Power Syst Res 201:107564

Ahmadi B, Ceylan O, Ozdemir A (2019a) Grey wolf optimizer for allocation and sizing of distributed renewable generation. In: 2019 54th international universities power engineering conference (UPEC), pp 1–6, September

Ahmadi B, Ceylan O, Ozdemir A (2019b) Optimal allocation of multi-type distributed generators for minimization of power losses in distribution systems. In: the 20th international conference on intelligent systems applications to power systems, ISAP 2019, New Delhi/India, December

Arabi Nowdeh S, Faraji Davoudkhani I, Moghaddam MJH, Seifi Najmi E, Abdelaziz AY, Ahmadi A, Razavi SE, Gandoman FH (2019) Fuzzy multi-objective placement of renewable energy sources in distribution system with objective of loss reduction and reliability improvement using a novel hybrid method. Appl Soft Comput 77:761–779

Asef F, Majidnezhad V, Feizi-Derakhshi M-R, Parsa S (2021) Heat transfer relation-based optimization algorithm (htoa). Soft Comput, pp 1–30

Baran ME, Wu FF (1989) Network reconfiguration in distribution systems for loss reduction and load balancing. IEEE Trans Power Delivery 4(2):1401–1407

Bavarsad Salehpoor I, Molla-Alizadeh-Zavardehi S (2019) A constrained portfolio selection model at considering risk-adjusted measure by using hybrid meta-heuristic algorithms. Appl Soft Comput 75:233–253

Biswas PP, Mallipeddi R, Suganthan PN, Amaratunga GAJ (2017) A multiobjective approach for optimal placement and sizing of distributed generators and capacitors in distribution network. Appl Soft Comput 60:268–280

Boveiri HR, Elhoseny M (2018) A-coa: an adaptive cuckoo optimization algorithm for continuous and combinatorial optimization. Neural Comput Appl 93:1–25

Brest J, Maučec MS, Bošković B (2019) The 100-digit challenge: Algorithm jde100. In: 2019 IEEE congress on evolutionary computation (CEC). IEEE 93:19–26

Burke EK, Kendall G et al (2005) Search methodologies. Springer, Berlin
Ceylan O (2020) Multi-verse optimization algorithm-and salp swarm optimization algorithm-based optimization of multilevel inverters. Neural Comput Appl 93:1–16
Chu X, Cai F, Gao D, Li L, Cui J, Xiu SX, Qin Q (2020) An artificial bee colony algorithm with adaptive heterogeneous competition for global optimization problems. Appl Soft Comput 93:106391
Eberhart R, Kennedy JS (1995) A new optimizer using particle swarm theory. MHS'95. In: Proceedings of the sixth international symposium on micro machine and human science, pp 39–43
Elaziz MA, Heidari AA, Fujita H, Moayedi H (2020) A competitive chain-based harris hawks optimizer for global optimization and multi-level image thresholding problems. Appl Soft Comput 37:106347
Eminoglu U, Hocaoglu M (2009) Distribution systems forward/backward sweep-based power flow algorithms: A review and comparison study. Elect Power Comp Syst 37(91–110):01
Geem ZW, Kim JH, Loganathan GV (2001) A new heuristic optimization algorithm: Harmony search. SIMULATION 76(2):60–68
Gnana Sundari M, Rajaram M, Balaraman S (2016) Application of improved firefly algorithm for programmed pwm in multilevel inverter with adjustable dc sources. Appl Soft Comput 41:169–179
Guner S, Ozdemir A (2020) Reliability improvement of distribution system considering ev parking lots. Elect Power Syst Res 185:106353
Gupta S, Deep K (2020) A memory-based grey wolf optimizer for global optimization tasks. Appl Soft Comput 93:106367
Heidari AA, Pahlavani P (2017) An efficient modified grey wolf optimizer with levy flight for optimization tasks. Appl Soft Comput 60:115–134
Heidari AA, Pahlavani P (2017) An efficient modified grey wolf optimizer with lévy flight for optimization tasks. Appl Soft Comput 60:115–134
Kansal V, Dhillon JS (2020) Emended salp swarm algorithm for multiobjective electric power dispatch problem. Appl Soft Comput 90:106172
Karthikumar K, Kumar VS (2021) A new opposition crow search optimizer-based two-step approach for controlled intentional islanding in microgrids. Soft Comput 25(4):2575–2588
Ke Q, Zhang J, Wei W, Połap D, Woźniak M, Kośmider L, Damaševĭcius R (2019) A neuro-heuristic approach for recognition of lung diseases from x-ray images. Expert Syst Appl 126:218–232
Khandelwal A, Bhargava A, Sharma A, Sharma H (2018) Modified grey wolf optimization algorithm for transmission network expansion planning problem. Arab J Sci Eng 43(6):2899–2908
Khodr HM, Olsina FG, De Oliveira-De Jesus PM, Yusta JM (2008) Maximum savings approach for location and sizing of capacitors in distribution systems. Elect Power Syst Res 78(7):1192–1203
Liu K, Sheng W, Liu Y, Meng X, Liu Y (2015) Optimal sitting and sizing of dgs in distribution system considering time sequence characteristics of loads and dgs. Int J Elect Power Energy Syst 69:430–440
Mahdad B, Srairi K (2015) Blackout risk prevention in a smart grid based flexible optimal strategy using grey wolf-pattern search algorithms. Energy Convers Manage 98:411–429
Mahesh A, Sushnigdha G (2021) A novel search space reduction optimization algorithm. Soft Comput, pp 1–28
Mirjalili S (2015) How effective is the grey wolf optimizer in training multi-layer perceptrons. Appl Intell 43(1):150–161
Mirjalili S (2015) Moth-flame optimization algorithm: A novel nature-inspired heuristic paradigm. Knowl-Based Syst 89:228–249
Mirjalili S (2015) The ant lion optimizer. Adv Eng Softw 83:80–98
Mirjalili S (2016) Sca: a sine cosine algorithm for solving optimization problems. Knowl-Based Syst 96:120–133
Mirjalili S, Mirjalili SM, Lewis A (2014) Grey wolf optimizer. Adv Eng Softw 69:46–61
Mirjalili S, Saremi S, Mirjalili SM, Coelho LS (2016) Multi-objective grey wolf optimizer: a novel algorithm for multi-criterion optimization. Expert Syst Appl 47:106–119
Mirjalili S, Mirjalili SM, Hatamlou A (2016) Multi-verse optimizer: a nature-inspired algorithm for global optimization. Neural Comput Appl 27(2):495–513
Mirjalili S, Gandomi AH, Mirjalili SZ, Saremi S, Faris H, Mirjalili SM (2017) Salp swarm algorithm: a bio-inspired optimizer for engineering design problems. Adv Eng Softw 114:163–191
Nguyen TP, Vo DN (2018) A novel stochastic fractal search algorithm for optimal allocation of distributed generators in radial distribution systems. Appl Soft Comput 70:773–796
Nguyen H, Moayedi H, Foong LK, Husam AH, Najjar A, Jusoh WAW, Rashid ASA, Jamali J (2020) Optimizing ANN models with PSO for predicting short building seismic response. Eng Comput 36(3):823–837
Papadimitrakis M, Giamarelos N, Stogiannos M, Zois EN, Livanos NA-I, Alexandridis A (2021) Metaheuristic search in smart grid: a review with emphasis on planning, scheduling and power flow optimization applications. Renew Sustain Energy Rev 145:111072
Pfenninger S, Staffell I (2016) Long-term patterns of european pv output using 30 years of validated hourly reanalysis and satellite data. Energy 114:1251–1265
Premkumar K, Manikandan BV (2015) Speed control of brushless dc motor using bat algorithm optimized adaptive neuro-fuzzy inference system. Appl Soft Comput 32:403–419
Price KV, Awad NH, Ali MZ, Suganthan PN (2018) The 100-digit challenge: Problem definitions and evaluation criteria for the 100-digit challenge special session and competition on single objective numerical optimization. Nanyang Technological University
Qin AK, Huang VL, Suganthan PN (2009) Differential evolution algorithm with strategy adaptation for global numerical optimization. IEEE Trans Evol Comput 13(2):398–417
Rahmani R, Langeroudi NMA, Yousefi R, Mahdian M, Seyedmahmoudian M (2014) Fuzzy logic controller and cascade inverter for direct torque control of im. Neural Comput Appl 25(3–4):879–888
Rashid TA, Abbas DK, Turel YK (2019) A multi hidden recurrent neural network with a modified grey wolf optimizer. PLoS ONE 14(3):1–23, 03
Saha A, Bhattacharya A, Das P, Chakraborty AK (2020) Hsos: a novel hybrid algorithm for solving the transient-stability-constrained opf problem. Soft Comput 24(10):7481–7510
Saha S, Mukherjee V (2020) A novel multi-objective modified symbiotic organisms search algorithm for optimal allocation of distributed generation in radial distribution system. Neural Comput Appl 83:1–21
Salgotra R, Singh U, Sharma S (2019) On the improvement in grey wolf optimization. Neural Comput Appl 36:1–40
Sanjay R, Jayabarathi T, Raghunathan T, Ramesh V, Mithulananthan N (2017) Optimal allocation of distributed generation using hybrid grey wolf optimizer. IEEE Access 5:14807–14818
Saremi S, Mirjalili SZ, Mirjalili SM (2015) Evolutionary population dynamics and grey wolf optimizer. Neural Comput Appl 26(5):1257–1263
Shehab M, Abualigah L, Hamad HA, Alabool H, Alshinwan M, Khasawneh AM (2019) Moth-flame optimization algorithm: variants and applications. Neural Comput Appl 33:1–26
Staffell I, Pfenninger S (2016) Using bias-corrected reanalysis to simulate current and future wind power output. Energy 114:1224–1239
Sultana U, Khairuddin AB, Mokhtar AS, Zareen N, Sultana B (2016) Grey wolf optimizer based placement and sizing of multiple distributed generation in the distribution system. Energy 111:525–536

Tolba Mohamed A, Hegazy R, Mujahed A-D, Eisa Ayman A (2020) Heuristic optimization techniques for connecting renewable distributed generators on distribution grids. Benefits 3:6

Trelea IC (2003) The particle swarm optimization algorithm: convergence analysis and parameter selection. Inf Process Lett 85(6):317–325

Truong KH, Nallagownden P, Elamvazuthi I, Vo DN (2019) An improved meta-heuristic method to maximize the penetration of distributed generation in radial distribution networks. Neural Comput Appl, pp 1–23

Truong KH, Nallagownden P, Elamvazuthi I, Dieu NV (2020) A quasi-oppositional-chaotic symbiotic organisms search algorithm for optimal allocation of dg in radial distribution networks. Appl Soft Comput 88:106067

Whitley D (1994) A genetic algorithm tutorial. Stat Comput 4:65–85

Yammani C, Maheswarapu S, Matam SK (2016) A multi-objective shuffled bat algorithm for optimal placement and sizing of multi distributed generations with different load models. Int J Elect Power Energy Syst 79:120–131

Yang B, Zhang X, Tao Yu, Shu H, Fang Z (2017) Grouped grey wolf optimizer for maximum power point tracking of doubly-fed induction generator based wind turbine. Energy Convers Manage 133:427–443

Yang X, Deb S (2009) Cuckoo search via lévy flights. In: 2009 world congress on nature biologically inspired computing (NaBIC), pp 210–214

Yeh J-F, Chen T-Y, Chiang T-C (2019) Modified l-shade for single objective real-parameter optimization. In: 2019 IEEE congress on evolutionary computation (CEC). IEEE, pp 381–386

Zhu A, Xu C, Li Z, Wu J, Liu Z (2015) Hybridizing grey wolf optimization with differential evolution for global optimization and test scheduling for 3d stacked soc. J Syst Eng Electron 26(2):317–328